

# Vibration of a rotary FG plate with consideration of thermal and Coriolis effects

Majid Ghadiri<sup>\*</sup>, Navvab Shafiei<sup>a</sup> and Ramin Babaei<sup>b</sup>

Department of Mechanical Engineering, Faculty of Engineering, Imam Khomeini International University, 3414916818, Qazvin, Iran

(Received May 09, 2016, Revised February 05, 2017, Accepted July 13, 2017)

**Abstract.** In this paper, Coriolis effect on vibration behavior of a rotating rectangular plate made of functionally graded (FG) materials under thermal loading has been investigated. The material properties of the FG plate are supposed to get changed in parallel with the thickness of the plate and the thermal properties of the material are assumed to be thermo-elastic. In this research, the effect of hub size, rotating speed and setting angle are considered. Governing equation of motion and the associated boundary conditions are obtained by Hamilton's principle. Generalized differential quadrature method (GDQM) is used to solve the governing differential equation with respect to cantilever boundary condition. The results were successfully verified with the published literatures. These results can be useful for designing rotary systems such as turbine blades. In this work, Coriolis and thermal effects are considered for the first time and GDQM method has been used in solving the equations of motion of a rotating FGM plate.

**Keywords:** functionally graded plate; vibration; Coriolis effect; thermal environment; GDQM method

## 1. Introduction

In last years, many researchers have studied different characteristics of plates. FGM plates are one of the newest mechanical structures with excellent mechanical properties. Functionally graded materials are intelligent composites that their material properties are changed continuously through specific directions of the structure (mostly in thickness direction) to reach desired properties. Functionally graded materials are often made of metal (due to unique mechanical properties) and ceramic (due to unique thermal properties). FGMs with a mixture of ceramic and metal are used as thermal barrier structures in aerospace shuttles, combustion chambers and nuclear plants and etc. (Park and Kim 2006). In another study, Bernardo *et al.* (2016) are presented various structural models and the performance of their developed models are carried out through a set of illustrative cases based on the survey of static and free vibration behavior of plates. A dynamic model of a functionally graded rectangular plate imposed by large overall motions is presented by Li and Zhang (2016). Ketabdari *et al.* (2016) studied free vibration of homogeneous and functionally graded skew plates resting on Winkler-Pasternak elastic foundation. Parametric resonance characteristics of FG plates on the elastic foundation which is proposed under biaxial in-plane periodic loads are presented by Ramu and Mohanty (2015). Prakash *et al.* (2015) studied large amplitude flexural vibration characteristics of FGM plates. Isogeometric analysis with non-uniform rational B-spline (NURBS) based on the classical plate theory (CPT) is developed for free vibration

analysis of thin functionally graded material (FGM) plates by Yin *et al.* (2013).

Nowadays, functionally graded materials are widely used in production of turbine blades. The failure in blades of compressors and turbines is happened mostly due to blade vibrations. Vibration of rotating blades plays an important role in designing many machines. One of the important purposes of this research is to help researchers find proper ways to design thinner blades which can operate in higher speeds. Thick blades which have large aspect ratios can be modeled as beams, plates or shells. Previous researches on rotating blades, dealt with the extraction of natural frequencies and mode shapes of blades rotating at a constant angular velocity. There are a few researches on the influence of external forces or damped vibrations in their rotating condition. Wang *et al.* (1987) are studied free vibration of a rectangular plate by considering the rotating velocity and the setting angle. Young and Liou (1992) studied the impact of Coriolis effect on vibration of a cantilever plate with a time-varying rotating speed. Vibration control of rotating blades using a root-embedded piezoelectric material is studied by Malgaca *et al.* (2015). The influence of Coriolis effect on the first bending and the first torsional frequencies of flat rotating low aspect ratio cantilever plates have been investigated by Sreenivasamurthy and Ramamurti (1981b). They have determined the natural frequencies of a pre-twisted and tapered plate mounted on the periphery of a rotating disc (Sreenivasamurthy and Ramamurti 1981a). Subrahmanyam and his colleagues (Subrahmanyam and Kaza 1986) examined the effects of pre-twist, pre-cone, setting angle and Coriolis forces on vibration and buckling behavior of rotating torsional rigid cantilevered beams. Modal characteristics of a rotating cantilever plate and also a dynamic modelling method for rectangular plates

\*Corresponding author, Ph.D.,  
E-mail: [ghadiri@eng.ikiu.ac.ir](mailto:ghadiri@eng.ikiu.ac.ir)

undergoing prescribed overall motion are investigated by Yoo and Pierre (2003). Houang and Soedel (1987) worked on the effects of Coriolis acceleration on free and forced in-plane vibrations of rotating rings on elastic foundation. Wang *et al.* showed theoretically that when the plate is electrically driven into thickness-shear vibration in one of the two in-plane directions of plate rotating around the plate normal, the Coriolis force due to rotation causes a thickness-shear vibration in a perpendicular direction with an electrical output (Wang *et al.* 2015a) and in another paper, they showed that, topological order and vibrational edge modes can exist in a classical mechanical system consisting of a two-dimensional honeycomb lattice of masses and springs (Wang *et al.* 2015b). A dynamic model of a functionally graded rectangular rotating plate undergoing large overall motions is presented by Li and Zhang (2016).

A layerwise finite element formulation has been presented by Pandey and Pradyumna (2015) for dynamic analysis of two types of FG sandwich plates with nonlinear temperature variation along the thickness; FGs have temperature dependent material properties. Thermal vibration study of magnetostrictive FG plate under rapid heating is computed by using the generalized differential quadrature (GDQM) method presented by Hong (2012).

In the current research, vibration characteristics of functionally graded rotating plates subjected to thermal loadings are demonstrated. Thermal properties of materials are intended as thermo-elastic and non-classical governing equation and related boundary conditions are derived by Hamilton's principle. To solve the governing equation, GDQM is used. The cantilever (clamped at  $x = 0$ , free at  $x = L$ , free at  $y = 0$ , free at  $y = b$ ) boundary conditions are considered. These boundary conditions make a special case in which vibration behavior of the plate in fundamental frequency is different from the behavior of the plate vibrating with higher mode of frequency. In addition, the effect of various parameters such as aspect ratio, twist angle, angular velocity, temperature change, mode number and FG index on vibration behavior of plates has been studied and the results are presented by figures and tables. Results show a good agreement, at the same special state, with past investigations especially with experimental results

by Lessia (1969) and analytical results by Wang *et al.* (1987) that are fundamental researches in the field of plate's vibrations. In above mentioned works, Coriolis and thermal effects had not been taken into account. In addition, using GDQM method in this present work is different from those works. The results of these studies, especially vibration behaviors of structures are very important and useful for engineers.

## 2. Preliminaries

### 2.1 FGM plates

In Fig. 1, a FGM plate with the length of  $a$ , width of  $b$  and thickness of  $h$ , made of both ceramics and metal is shown. The materials at the bottom surface ( $Z = -h/2$ ) and the top surface ( $Z = h/2$ ) of this structure are metal and ceramic. The local effective material properties of the FGM plate can be calculated by the power law approach. Based on the Power-law approach, the effective properties of functionally graded plates involving Young's modulus ( $E$ ), Poisson's ratio ( $\nu$ ), mass density ( $\rho$ ) and thermal expansion coefficient ( $\alpha$ ) can be written as follows

$$E(z) = E_c V_c(z) + E_m V_m \tag{1}$$

$$\nu(z) = \nu_c V_c(z) + E \nu_m V_m \tag{2}$$

$$\rho(z) = \rho_c V_c(z) + \rho_m V_m \tag{3}$$

$$\alpha(z) = \alpha_c V_c(z) + \alpha_m V_m \tag{4}$$

Now, the indexes  $m$  and  $c$  refer to metal and ceramic phases, respectively. The volume fraction of ceramic and metal phases can be shown based on the power-law function as

$$V_f(z) = \left(\frac{1}{2} + \frac{z}{h}\right)^k \tag{5}$$

where,  $k$  represents the power-law index. Additionally, the neutral axis of the FGM plate where the end supports are located on, can be determined by the following relation (Young and Liou 1992)

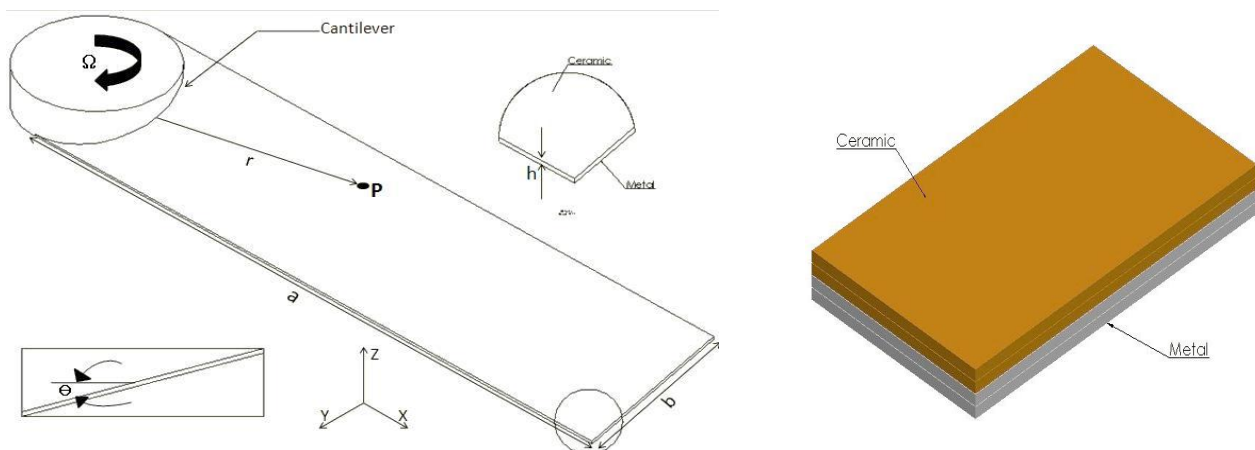


Fig. 1 Geometrical position and boundary condition of the rotating FGM plate

$$z_0 = \frac{\int_{-(h/2)}^{(h/2)} zE(z)dz}{\int_{-(h/2)}^{(h/2)} E(z)dz} \quad (6)$$

### 3. Formulation

The displacement field of the classical plate along  $x$ ,  $y$  and  $z$ -directions can be written as

$$u_x = -z \frac{\partial W}{\partial x}, \quad u_y = -z \frac{\partial W}{\partial y}, \quad u_z = W(x, y, t) \quad (7)$$

where,  $W$  stands for transverse deformation of the plate. The required components of the strain tensor can be obtained as

$$\varepsilon_{xx} = -z \frac{\partial^2 W}{\partial x^2}, \quad \varepsilon_{yy} = -z \frac{\partial^2 W}{\partial y^2}, \quad \varepsilon_{xy} = -2z \frac{\partial^2 W}{\partial x \partial y} \quad (8)$$

Based on elasticity theory, the related components of stress tensor for the bulk plate can be calculated by the Hook's law as follows

$$\begin{aligned} \sigma_{xx} &= \frac{E}{1-\nu^2} (\varepsilon_{xx} + \nu \varepsilon_{yy}) \\ &= -\frac{Ez}{1-\nu^2} \left( \frac{\partial^2 W}{\partial x^2} + \nu \frac{\partial^2 W}{\partial y^2} \right) \end{aligned} \quad (9)$$

$$\begin{aligned} \sigma_{yy} &= \frac{E}{1-\nu^2} (\varepsilon_{yy} + \nu \varepsilon_{xx}) \\ &= -\frac{Ez}{1-\nu^2} \left( \frac{\partial^2 W}{\partial y^2} + \nu \frac{\partial^2 W}{\partial x^2} \right) \end{aligned} \quad (10)$$

$$\sigma_{xy} = \frac{E}{2(1+\nu)} \varepsilon_{xy} = -\frac{Ez}{(1+\nu)} \frac{\partial^2 W}{\partial x \partial y} \quad (11)$$

According to the continuum surface elasticity theory, the related strain energy of this plate imposed by surface stress can be formulated as

$$U = \frac{1}{2} \int_A \int_{-(h/2)}^{(h/2)} \sigma_{ij} \varepsilon_{ij} dz dA \quad (12)$$

Plate rotates with the constant angular velocity,  $\Omega$ . Considering an arbitrary point,  $P$ , in the middle of the plane, the absolute position of  $P$  can be represented as follows

$$r_p = r_0 + r + d \quad (13)$$

In which  $d = u\hat{i} + v\hat{j} + w\hat{k}$ ,  $r_0 + r = R_1\hat{i} + R_2\hat{j} + R_3\hat{k}$ ; the definition of angular velocity is  $\Omega = \Omega_1\hat{i} + \Omega_2\hat{j} + \Omega_3\hat{k}$ .

To escape from a difficult computational problem-solving procedure, we assume that  $R_i$  and  $\Omega_i$  are constant.

The absolute velocity of the point  $P$  includes three following terms

$$v_p = \frac{\partial d}{\partial t} + \Omega \times d + \Omega \times (r_0 + r) \quad (14)$$

The first term is due to displacement, the second term is

caused by angular rotation and the last one shows relative axis rotation. Neglecting the rotary inertia, this velocity provides the kinetic energy. The kinetic energy can be written in four statements as follows

$$P_1 = \frac{1}{2} \int_V \rho \left[ \left( \frac{\partial w}{\partial t} \right)^2 + z \left( \frac{\partial^2 w}{\partial x \partial t} \right)^2 + z \left( \frac{\partial^2 w}{\partial y \partial t} \right)^2 \right] dV \quad (15)$$

$$\begin{aligned} P_2 &= \frac{1}{2} \int_V \rho [(\Omega \times d) \cdot (\Omega \times d)] dV \\ &= \int_V \rho \left[ (\Omega_1 + \Omega_2)w^2 + (\Omega_1 + \Omega_3)z^2 \left( \frac{\partial w}{\partial y} \right)^2 \right. \\ &\quad \left. (\Omega_2 + \Omega_3)z^2 \left( \frac{\partial w}{\partial x} \right)^2 - 2\Omega_2\Omega_3zw \left( \frac{\partial w}{\partial y} \right) \right. \\ &\quad \left. - 2\Omega_1\Omega_3zw \left( \frac{\partial w}{\partial x} \right) - 2\Omega_1\Omega_2 \left( \frac{\partial w}{\partial x} \right) \left( \frac{\partial w}{\partial y} \right) \right] dV \end{aligned} \quad (16)$$

$$\begin{aligned} P_3 &= \int_A \left[ \rho(\Omega \times d) \cdot \left( \frac{\partial d}{\partial t} \right) \right] dV \\ &= \int_A \left[ \left[ I_1 \left( \Omega_1 \left( \frac{\partial w}{\partial y} \cdot \frac{\partial w}{\partial t} \right) + \Omega_2 \left( \frac{\partial w}{\partial x} \cdot \frac{\partial w}{\partial t} \right) \right. \right. \right. \\ &\quad \left. \left. + \Omega_2 \left( w \cdot \frac{\partial^2 w}{\partial x \partial t} \right) + \Omega_1 \left( w \cdot \frac{\partial^2 w}{\partial y \partial t} \right) \right] \right. \\ &\quad \left. + \left[ I_2 \left( \Omega_3 \left( \frac{\partial^2 w}{\partial x \partial t} \cdot \frac{\partial w}{\partial y} \right) + \Omega_3 \left( \frac{\partial^2 w}{\partial y \partial t} \cdot \frac{\partial w}{\partial x} \right) \right) \right] \right] dA \end{aligned} \quad (17)$$

$$U_g = \frac{1}{2} \left[ N_x^0 \left( \frac{\partial w}{\partial x} \right)^2 + 2N_{xy}^0 \left( \frac{\partial w}{\partial x} \cdot \frac{\partial w}{\partial y} \right) + N_y^0 \left( \frac{\partial w}{\partial y} \right)^2 \right] \quad (18)$$

In which,  $[I_0, I_1, I_2]$  are defined in the following equation

$$[I_0, I_1, I_2] = \int_{-(h/2)}^{(h/2)} \rho [1, z, z^2] dz \quad (19)$$

The first statement shows the kinetic energy of vibrational motion. The second statement shows the work done by displacements related to centrifugal forces and the third statement exhibits the work done by displacements related to Coriolis forces which plays an important role in this research. Last statement shows the work done by independent-displacement centrifugal forces.

Also, the work done by the external forces can be calculated as

$$W_{ext} = \int_A \left[ N_{Tx} \left( \frac{\partial W}{\partial x} \right)^2 + N_{Ty} \left( \frac{\partial W}{\partial y} \right)^2 \right] dA \quad (20)$$

in which

$$N_{Tx} = \int_{-(h/2)}^{(h/2)} \sigma_{xx}^T dz, \quad N_{Ty} = \int_{-(h/2)}^{(h/2)} \sigma_{yy}^T dz \quad (21)$$

Thermal loading is applied along the neutral axis. These forces cause the axial stress as follows

$$\sigma_{xx}^T = -\frac{E\alpha(T - T_0)}{1 - \nu} \quad (22)$$

$T_0$  is the initial uniform temperature of a stress free state that it is assumed as 300 K.

$$\int_{t_1}^{t_2} (\delta K - \delta U + \delta W_{ext}) dt = 0 \quad (23)$$

Taking the variation of  $w$  and integrating by part, the equations of motion and the boundary conditions will be obtained by setting the coefficient of  $\delta w$  equal to zero based on the fundamental lemma as follows

$$\begin{aligned} \delta U &= \int_A \left[ M_{xx} \delta \left( \frac{\partial^2 W}{\partial x^2} \right) + M_{yy} \delta \left( \frac{\partial^2 W}{\partial y^2} \right) \right. \\ &\quad \left. + M_{xy} \delta \left( \frac{\partial^2 W}{\partial x \partial y} \right) + M_{xy} \delta \left( \frac{\partial^2 W}{\partial y \partial x} \right) \right] dA \\ &= -M_{xx} \delta \left[ \frac{\partial w}{\partial x} \right]_0^a + \frac{\partial M_{xx}}{\partial x} [\delta w]_0^a - \int_A \frac{\partial^2 M_{xx}}{\partial x^2} \delta w dA \\ &\quad - M_{yy} \delta \left[ \frac{\partial w}{\partial y} \right]_0^b + \frac{\partial M_{yy}}{\partial y} [\delta w]_0^b - \int_A \frac{\partial^2 M_{yy}}{\partial y^2} \delta w dA \\ &\quad - M_{xy} \delta \left[ \frac{\partial w}{\partial y} \right]_0^a + \frac{\partial M_{xy}}{\partial x} \delta [w]_0^b - \int_A \frac{\partial^2 M_{xy}}{\partial x \partial y} \delta w dA \\ &\quad - M_{xy} \delta \left[ \frac{\partial w}{\partial x} \right]_0^b + \frac{\partial M_{xy}}{\partial y} \delta [w]_0^a - \int_A \frac{\partial^2 M_{xy}}{\partial x \partial y} \delta w dA \end{aligned} \quad (24)$$

in which

$$\{M_{xx}, M_{yy}, M_{xy}\}^T = \int_{-(h/2)}^{(h/2)} \{\sigma_{xx} z, \sigma_{yy} z, \sigma_{xy} z\}^T dz \quad (25)$$

The kinetic energy can be written as

$$\begin{aligned} \delta P_1 &= - \int_A I_0 \frac{\partial^2 w}{\partial t^2} \delta w dA + I_1 \frac{\partial^3 w}{\partial x \partial t^2} \delta [w]_0^a \\ &\quad - \int_A I_1 \frac{\partial^4 w}{\partial t^2 \partial x^2} \delta w dA + I_1 \frac{\partial^3 w}{\partial y \partial t^2} \delta [w]_0^b \\ &\quad - \int_A I_1 \frac{\partial^4 w}{\partial t^2 \partial y^2} \delta w dA \end{aligned} \quad (26)$$

$$\begin{aligned} \delta U_g &= N_x^0 \frac{\partial w}{\partial x} \delta [w]_0^a \\ &\quad - \int_A N_x^0 \frac{\partial^2 w}{\partial x^2} \delta w dA + N_y^0 \frac{\partial w}{\partial y} \delta [w]_0^b \\ &\quad - \int_A N_y^0 \frac{\partial^2 w}{\partial y^2} \delta w dA + N_{xy}^0 \frac{\partial w}{\partial x} \delta [w]_0^b \\ &\quad - \int_A N_{xy}^0 \frac{\partial^2 w}{\partial x \partial y} \delta w dA + N_{xy}^0 \frac{\partial w}{\partial y} \delta [w]_0^a \\ &\quad - \int_A N_{xy}^0 \frac{\partial^2 w}{\partial x \partial y} \delta w dA \end{aligned} \quad (27)$$

$$\begin{aligned} \delta P_2 &= \int_A I_0 (\Omega_1 + \Omega_2) w \delta w dA + I_2 (\Omega_1 + \Omega_3) \frac{\partial w}{\partial y} \delta [w]_0^b \\ &\quad - \int_A I_2 (\Omega_1 + \Omega_3) \frac{\partial^2 w}{\partial y^2} \delta w dA \\ &\quad + I_2 (\Omega_2 + \Omega_3) \frac{\partial w}{\partial x} \delta [w]_0^a \\ &\quad - \int_A I_2 (\Omega_2 + \Omega_3) \frac{\partial^2 w}{\partial x^2} \delta w dA \\ &\quad - 2 \int_A I_1 (\Omega_2 \Omega_3) \frac{\partial w}{\partial y} \delta w dA - 2 I_1 (\Omega_2 \Omega_3) w \delta [w]_0^b \\ &\quad + 2 \int_A I_1 (\Omega_2 \Omega_3) \frac{\partial w}{\partial y} \delta w dA \\ &\quad - 2 \int_A I_1 (\Omega_1 \Omega_3) \frac{\partial w}{\partial x} \delta w dA \\ &\quad - 2 I_1 (\Omega_1 \Omega_3) w \delta [w]_0^a + 2 \int_A I_1 (\Omega_1 \Omega_3) \frac{\partial w}{\partial x} \delta w dA \\ &\quad - 2 I_0 (\Omega_1 \Omega_2) \frac{\partial w}{\partial y} \delta [w]_0^a \\ &\quad + 2 \int_A I_0 (\Omega_1 \Omega_2) \frac{\partial^2 w}{\partial x \partial y} \delta w dA \\ &\quad - 2 I_0 (\Omega_1 \Omega_2) \frac{\partial w}{\partial x} \delta [w]_0^b \\ &\quad + 2 \int_A I_0 (\Omega_1 \Omega_2) \frac{\partial^2 w}{\partial x \partial y} \delta w dA \end{aligned} \quad (28)$$

$$\begin{aligned} \delta P_3 &= - \int_A I_1 \Omega_1 \frac{\partial^2 w}{\partial y \partial t} \delta w dA \\ &\quad - \int_A I_1 \Omega_2 \frac{\partial^2 w}{\partial x \partial t} \delta w dA + I_1 \Omega_1 \frac{\partial w}{\partial t} \delta [w]_0^b \\ &\quad - \int_A I_1 \Omega_1 \frac{\partial^2 w}{\partial y \partial t} \delta w dA + I_1 \Omega_2 \frac{\partial w}{\partial t} \delta [w]_0^a \\ &\quad - \int_A I_1 \Omega_2 \frac{\partial^2 w}{\partial x \partial t} \delta w dA - \int_A I_1 \Omega_2 \frac{\partial^2 w}{\partial x \partial t} \delta w dA \\ &\quad + \int_A I_1 \Omega_1 \frac{\partial^2 w}{\partial y \partial t} \delta w dA - \int_A I_1 \Omega_2 \frac{\partial^2 w}{\partial x^2} \delta w dA \\ &\quad + \int_A I_1 \Omega_1 \frac{\partial^2 w}{\partial y^2} \delta w dA + I_1 \Omega_2 \frac{\partial w}{\partial x} \delta [w]_0^a \\ &\quad - I_1 \Omega_1 \frac{\partial w}{\partial y} \delta [w]_0^b - I_2 \Omega_3 \frac{\partial^2 w}{\partial x \partial t} \delta [w]_0^b \\ &\quad + I_2 \Omega_3 \frac{\partial^2 w}{\partial y \partial t} \delta [w]_0^a + I_2 \Omega_3 \frac{\partial^2 w}{\partial y \partial t} \delta [w]_0^a \\ &\quad - I_2 \Omega_3 \frac{\partial^2 w}{\partial x \partial t} \delta [w]_0^b \end{aligned} \quad (29)$$

$$\begin{aligned} \delta W_{ext} &= N_{Tx} \frac{\partial w}{\partial x} \delta [w]_0^a - \int_A N_{Tx} \frac{\partial^2 w}{\partial x^2} \delta w dA \\ &\quad + N_{Ty} \frac{\partial w}{\partial y} \delta [w]_0^b - \int_A N_{Ty} \frac{\partial^2 w}{\partial y^2} \delta w dA \end{aligned} \quad (30)$$

After the above steps, to obtain the governing equation

$$\begin{bmatrix} M_{xx} \\ M_{yy} \\ M_{xy} \end{bmatrix} = \begin{bmatrix} D_{11} & D_{12} & 0 \\ D_{21} & D_{22} & 0 \\ 0 & 0 & D_{66} \end{bmatrix} \begin{bmatrix} \frac{\partial^2 w}{\partial x^2} \\ \frac{\partial^2 w}{\partial y^2} \\ \frac{\partial^2 w}{\partial x \partial y} \end{bmatrix}; \begin{bmatrix} D_{11} & D_{12} & 0 \\ D_{21} & D_{22} & 0 \\ 0 & 0 & D_{66} \end{bmatrix} \quad (31)$$

$$= \int_{-(h/2)}^{(h/2)} \begin{bmatrix} -\frac{E(z)z^2}{1-\nu^2} & -\frac{E(z)z^2\nu}{1-\nu^2} & 0 \\ \frac{E(z)z^2\nu}{1-\nu^2} & -\frac{E(z)z^2}{1-\nu^2} & 0 \\ 0 & 0 & -\frac{E(z)z^2}{(1+\nu)} \end{bmatrix} dz$$

And the governing equation is as follows

$$\begin{aligned} & D_{11} \frac{\partial^4 w}{\partial x^4} + (D_{12} + D_{21} + 2D_{66}) \frac{\partial^4 w}{\partial x^2 \partial y^2} + D_{22} \frac{\partial^4 w}{\partial y^4} \\ & + N_x^0 \frac{\partial^2 w}{\partial x^2} + N_y^0 \frac{\partial^2 w}{\partial y^2} + 2N_{xy}^0 \frac{\partial^2 w}{\partial x \partial y} + N_{Tx} \frac{\partial^2 w}{\partial x^2} \\ & + N_{Ty} \frac{\partial^2 w}{\partial y^2} + I_2(\Omega_1 + \Omega_3) \frac{\partial^2 w}{\partial y^2} + I_2(\Omega_2 + \Omega_3) \frac{\partial^2 w}{\partial x^2} \\ & + I_1 \Omega_2 \frac{\partial^2 w}{\partial x^2} - I_1 \Omega_1 \frac{\partial^2 w}{\partial y^2} + 2I_0(\Omega_1 \Omega_2) \frac{\partial^2 w}{\partial x \partial y} \\ & + I_0(\Omega_1 + \Omega_2)w = I_0 \frac{\partial^2 w}{\partial t^2} + 2I_1 \Omega_1 \frac{\partial^2 w}{\partial y \partial t} + 2I_1 \Omega_2 \frac{\partial^2 w}{\partial x \partial t} \\ & + I_1 \frac{\partial^4 w}{\partial t^2 \partial y^2} + I_1 \frac{\partial^4 w}{\partial t^2 \partial x^2} + I_1 \Omega_2 \frac{\partial^2 w}{\partial x \partial t} - I_1 \Omega_1 \frac{\partial^2 w}{\partial y \partial t} \end{aligned} \quad (32)$$

In the final step, assuming that  $\Omega_1 = \Omega_0 \cos \theta$ ,  $\Omega_2 = \Omega_0 \sin \theta$  and  $\Omega_3 = 0$

$$\begin{aligned} & D_{11} \frac{\partial^4 w}{\partial x^4} + 2(D_{21} + D_{66}) \frac{\partial^4 w}{\partial x^2 \partial y^2} + D_{22} \frac{\partial^4 w}{\partial y^4} \\ & + (N_x^0 + N_{Tx} + \Omega_0 I_2 \sin \theta + \Omega_0 I_1 \sin \theta) \frac{\partial^2 w}{\partial x^2} \\ & + (N_y^0 + N_{Ty} + \Omega_0 I_2 \cos \theta - \Omega_0 I_1 \sin \theta) \frac{\partial^2 w}{\partial y^2} \\ & + (2N_{xy}^0 + I_0 \Omega_0^2 \sin 2\theta) \frac{\partial^2 w}{\partial x \partial y} \\ & + (I_0 \Omega_0 (\sin \theta + \cos \theta))w \\ & = I_0 \frac{\partial^2 w}{\partial t^2} + 3I_1 \Omega_0 \cos \theta \frac{\partial^2 w}{\partial y \partial t} + 3I_1 \Omega_0 \sin \theta \frac{\partial^2 w}{\partial x \partial t} \\ & + I_1 \left( \frac{\partial^4 w}{\partial t^2 \partial y^2} + \frac{\partial^4 w}{\partial t^2 \partial x^2} \right) \end{aligned} \quad (33)$$

#### 4. Employing generalized differential quadrature method

In this section, generalized differential quadrature method (GDQM) is applied to governing equation to

calculate the spatial derivative of the field variable from the equilibrium equation. Recently, this method has been used by many researchers to analyze plates or beams behaviors (Shahrokhi *et al.* 2015, Ghadiri and Shafiei 2015, Tornabene *et al.* 2014, 2015a, b, Sofiyev 2015). In this method, grids suggest the locations of calculating derivatives and field variables. Derivative of the function with respect to a variable at an arbitrary node is equal to sum of the function values at all of nodes of mesh lines.

$$\left. \frac{\partial^r f(x)}{\partial x^r} \right|_{x=x,P} = \sum_{j=1}^n C_{ij}^{(r)} f(x_j) \quad (34)$$

In the above equation,  $n$  is the total number of discrete grid points in approximation and  $C_{ij}^{(r)}$  is the weighting coefficient. For example,  $C_{ij}^{(r)}$  is obtained from the first derivative which is defined as:

$$C_{ij}^{(1)} = \frac{M(x_i)}{(x_i - x_j)M(x_j)}, \quad (35)$$

$$i, j = 1, 2, \dots, n \quad \text{and} \quad i \neq j$$

In which

$$M(x_i) = \prod_{j=1, j \neq i}^n (x_i - x_j) \quad (36)$$

The equation of higher order derivate for weighting coefficient is shown below

$$C_{ij}^{(r)} = r \left[ C_{ij}^{(r-1)} C_{ij}^{(1)} \frac{C_{ij}^{(r-1)}}{(x_i - x_j)} \right] \quad (37)$$

$$i, j = 1, 2, \dots, n \quad \text{and} \quad i \neq j$$

$$C_{ii}^{(r)} = \sum_{j=1, j \neq i}^n C_{ij}^{(r)} \quad (38)$$

$$i, j = 1, 2, \dots, n \quad \text{and} \quad i = j$$

Selected grid points are along the coordinate axes direction at the computational domain. It carefully shows that the result of non-uniform grid points with the same number of spaced grid point is great. Thus, similar to this, choosing the set of grid points in natural coordinate directions of  $x$  and  $y$ , as shown in the figure of the plate, the length of plate in  $x$  direction is  $a$  and in the  $y$  direction is  $b$ . So

$$x_i = \frac{a}{2} \left( 1 - \cos \left( \frac{(i-1)\pi}{(n_i-1)} \right) \right) \quad (39)$$

$$y_i = \frac{b}{2} \left( 1 - \cos \left( \frac{(j-1)\pi}{(n_j-1)} \right) \right)$$

$$\zeta_i = \frac{1}{2} \left( 1 - \cos \left( \frac{(i-1)\pi}{(n_i-1)} \right) \right) \quad (40)$$

$$\eta_i = \frac{1}{2} \left( 1 - \cos \left( \frac{(j-1)\pi}{(n_j-1)} \right) \right)$$

Table 1 Comparison of the results for vibration of the classical plate with CFFF boundary conditions

	Mode number = 1	Mode number = 2	Mode number = 3	Mode number = 4
(Lessia 1969)	3.494	8.547	21.44	27.46
(Wang <i>et al.</i> 1987)	3.41	8.28	21.45	26.67
Present	3.454	8.866	22.366	28.265

Table 2 Comparison of the results for vibration of the FGM rotary plate with CFFF boundary conditions

	Fundamental frequency	Second frequency	Third frequency	Forth frequency	Fifth frequency
Yoo and Pierre 2003	13.273	15.311	29.792	43.289	48.851
Li and Zhang 2016	13.260	15.278	29.728	43.126	49.406
Present	13.221	15.345	30.571	43.594	49.811

Table 3 The temperature related properties of metal and ceramic phases for smart materials (Yang and Shen 2002)

Material	Properties	X <sub>0</sub>	X <sub>-1</sub>	X <sub>1</sub>	X <sub>2</sub>	X <sub>3</sub>
SUS304	E (Pa)	2.0104e+11	0	0.000308	-6.53e-07	0
	α(K <sup>-1</sup> )	1.23e-05	0	0.000809	0	0
	ρ (Kg/m <sup>3</sup> )	8166	0	0	0	0
	ν	0.3262	0	-0.0002	3.80e-07	0
Aluminum Oxid	E (Pa)	3.4955e+11	0	-0.0003853	4.027e-07	-1.673e-11
	α(K <sup>-1</sup> )	6.8269e-06	0	0.0001838	0	0
	ρ (Kg/m <sup>3</sup> )	3750	0	0	0	0
	ν	0.26	0	0	0	0

Assuming  $W$  as the following periodic form

$$w(x, y, t) = W(x, y)e^{i\omega t} \tag{41}$$

Substituting  $W$  in the equation of the motion, the governing equation of the rotating plate is calculated as

$$\begin{aligned}
 & D_{11} \sum_{k=1}^{n_j} C_{i,k}^{(4)} W_{k,j} \\
 & + (D_{12} + D_{21} + 2D_{66}) \sum_{k1=1}^{n_i} \sum_{k2=1}^{n_j} C_{i,k1}^{(2)} \bar{C}_{i,k2}^{(2)} W_{k1,k2} \\
 & + D_{22} \sum_{k=1}^{n_j} \bar{C}_{i,k}^{(4)} W_{i,k} \sum_{k=1}^{n_i} C_{i,k}^{(1)} \left( N_{xx} \sum_{k=1}^{n_i} C_{i,k}^{(1)} W_{k,j} \right) \\
 & + \sum_{k=1}^{n_j} \bar{C}_{i,k}^{(1)} \left( N_{yy} \sum_{k=1}^{n_j} \bar{C}_{i,k}^{(1)} W_{k,j} \right) \\
 & \sum_{k=1}^{n_i} C_{i,k}^{(1)} \left( \bar{N}_{xy} \sum_{k=1}^{n_j} \bar{C}_{i,k}^{(1)} W_{i,k} \right) \\
 & + \sum_{k=1}^{n_j} \bar{C}_{i,k}^{(1)} \left( N_{yy} \sum_{k=1}^{n_i} C_{i,k}^{(1)} W_{k,j} \right)
 \end{aligned} \tag{42}$$

$$\begin{aligned}
 & [I_2(\Omega_2 + \Omega_3) + I_1\Omega_2] \sum_{k=1}^{n_i} C_{i,k}^{(2)} W_{k,j} \\
 & + [I_2(\Omega_1 + \Omega_3) + I_1\Omega_1] \sum_{k=1}^{n_j} \bar{C}_{i,k}^{(1)} W_{i,k} (2I_0\Omega_2\Omega_1) \\
 & \sum_{k1=1}^{n_i} \sum_{k2=1}^{n_j} C_{i,k1}^{(1)} \bar{C}_{i,k2}^{(1)} W_{k1,k2} + I_0(\Omega_2 + \Omega_1)W_{i,j} \\
 & = \frac{\partial^2 \left( I_0W_{i,j} + I_1 \left( \sum_{k=1}^{n_i} C_{i,k}^{(1)} W_{k,j} + \sum_{k=1}^{n_j} \bar{C}_{i,k}^{(2)} W_{i,k} \right) \right)}{\partial t^2} \\
 & + \frac{\partial \left( I_1\Omega_1 \left( \sum_{k=1}^{n_j} \bar{C}_{i,k}^{(1)} W_{i,k} + 3I_1\Omega_2 \sum_{k=1}^{n_i} C_{i,k}^{(1)} W_{k,j} \right) \right)}{\partial t}
 \end{aligned} \tag{42}$$

where,  $C_{ij}^{(r)}$  and  $\bar{C}_{ij}^{(r)}$  are weighting coefficients associated with the  $r$ -th order derivative in  $x$ -and  $y$ -directions, respectively. Also,  $n_i$  and  $n_j$  stand for the numbers of total discrete grid points along  $x$  and  $y$  directions, respectively.

Now, boundary conditions and eigenvalues are applied to above equation to reach the final form for the solution as below

$$\begin{aligned}
 & \begin{bmatrix} [A_{bb}] & [A_{bi}] \\ [A_{ib}] & [A_{ii}] \end{bmatrix} \begin{Bmatrix} W_b \\ W_i \end{Bmatrix} \\
 & = \omega^2 \begin{bmatrix} 0 & 0 \\ [B_{ib}] & [B_{ii}] \end{bmatrix} \begin{Bmatrix} W_b \\ W_i \end{Bmatrix} + \omega \begin{bmatrix} 0 & 0 \\ [C_{ib}] & [C_{ii}] \end{bmatrix} \begin{Bmatrix} W_b \\ W_i \end{Bmatrix}
 \end{aligned} \tag{43}$$

where, the subscripts  $W_b$  and  $W_i$  refer to the boundary and domain grid points, respectively.

### 5. Results and discussion

Here, the results of numerical solutions for the transverse free vibration of the rotating FG plate are presented. The results are compared with previous results of other studies in several numerical examples to illustrate the accuracy of this work. In order to display the influence of plate important parameters such as the angular velocity, temperature change, FG-index and aspect ratio on various mode numbers, several figures and tables are presented. Non-dimensional parameters are defined as follows to make the analysis easier

$$r = \delta L; \quad \Phi^2 = \left(\frac{m_0}{EI}\right)_{ceramic} L^4 \Omega^2; \quad (44)$$

$$\Psi^2 = \left(\frac{m_0}{EI}\right)_{ceramic} L^4 \omega^2; \quad \left(\frac{m_0}{EI}\right)_{ceramic} = \frac{12\rho_{ceramic}}{E_{ceramic} h_1^2};$$

where,  $\Psi$ ,  $\Phi$  and  $\delta$  indicate non-dimensional frequency, non-dimensional angular velocity and non-dimensional hub radius, respectively.

Solving above equation can represent vibration behavior

of a plate rotating with a constant angular velocity around the vertical axis. This section shows the effect of different thermal changes, FG indexes, angular velocities and aspect ratios on the non-dimensional frequency. Firstly, we compared the classical plate vibration resulted from solving the above equation with the provided plate in this research with the same condition: cantilever boundary condition and various mode numbers. It shows a good agreement with previous experimental study by Lessia (1969) and analytical study by Wang *et al.* (1987). The results of this comparison are presented in Table 1.

In other comparison, the results of proposed method shows good accuracy with the results of previous work which are in the field of rectangular functionally graded plate's vibration by Li and Zhang (2016) and rectangular rotary plate's vibration by Yoo and Pierre (2003). This comparison is shown in Table. 2. And these results have been extracted for special non-dimensional angular velocity ( $\Phi = 10$ ) and special non-dimensional hub radius ( $\delta = 1$ ).

Mechanical properties of this plate is related to the temperature of both phases including metal and ceramic. These properties are assumed thermo-elastic and are related to the temperature. Following equation is presented for using these properties at various temperatures. Substituting the parameters of Table 3 into the mechanical properties equation, the properties in different temperatures can be

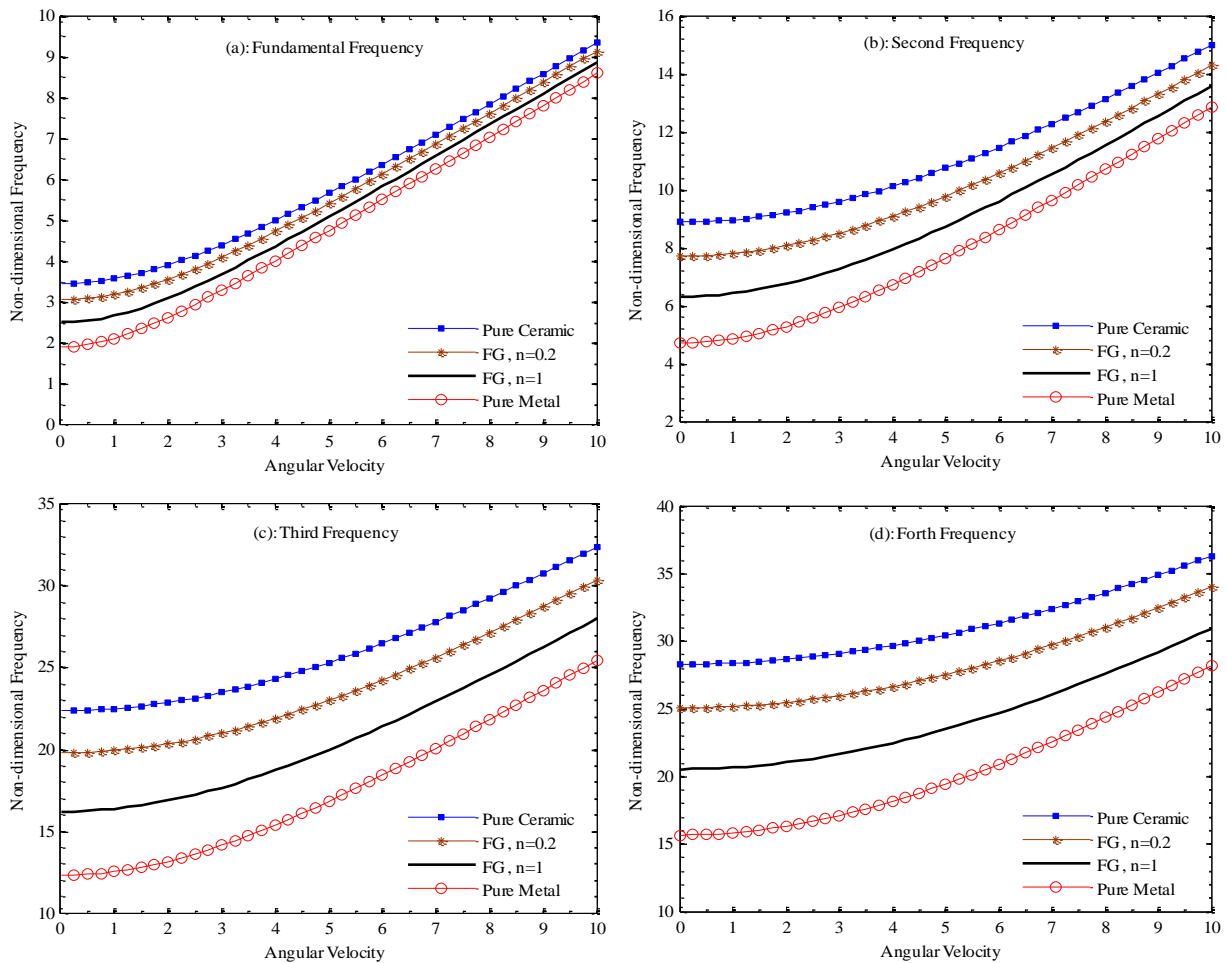


Fig. 2 The effect of various angular velocities on non-dimensional frequency in different FG indexes

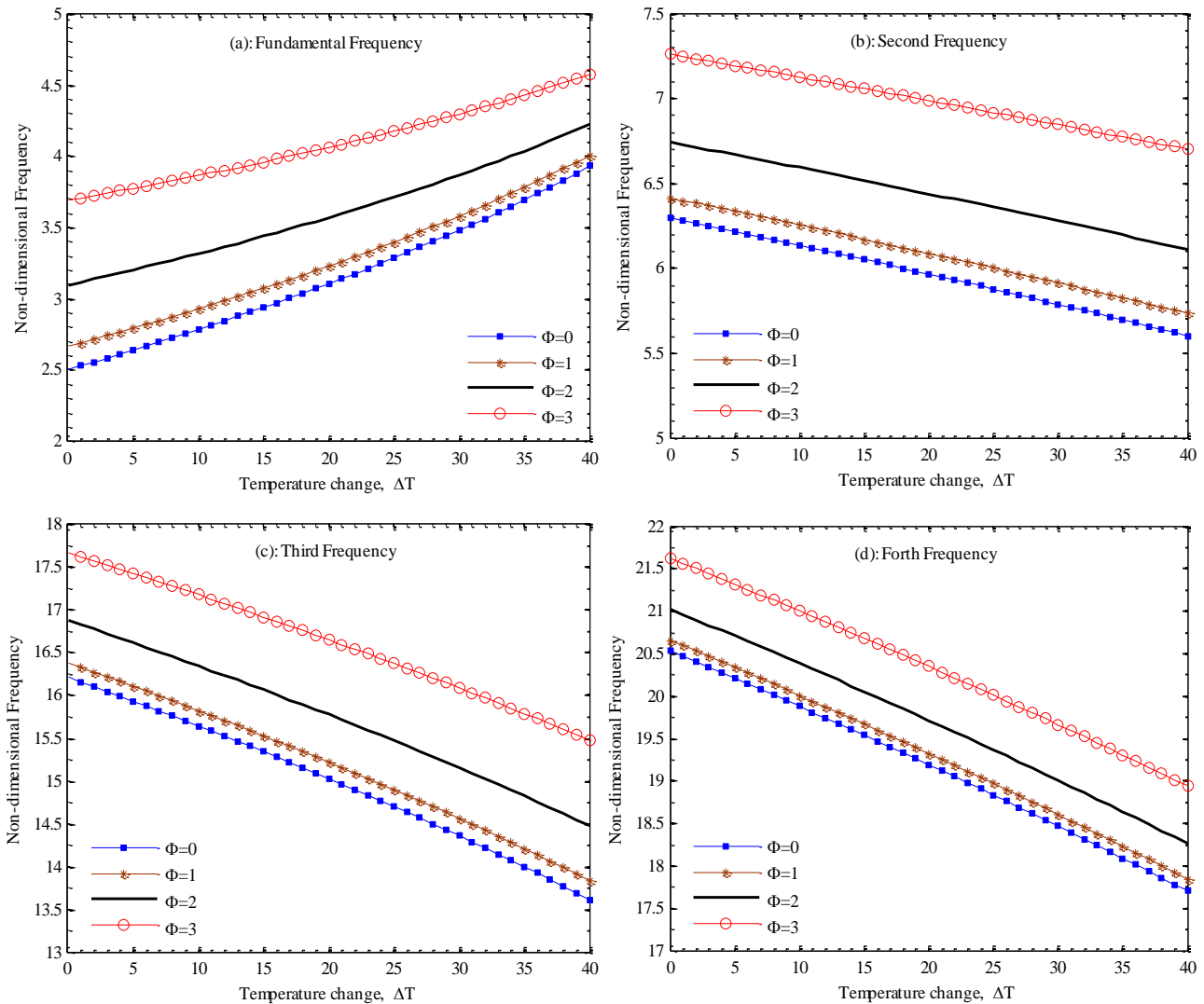


Fig. 3 The effect of various thermal changes on non-dimensional frequency at different angular velocities

calculated.  $T$  in this equation is the operating temperature of the system and shows the relation between material properties and temperature. Yang and Shen, presented these details in their previous study (Yang and Shen 2002)

$$X = X_0(X_{-1}T^{-1} + X_1T + X_2T^2 + X_3T^3 + 1) \quad (45)$$

Fig. 2 shows the effect of various angular velocities on the non-dimensional frequency of a functionally graded rotating plate. Different mode numbers from the fundamental frequency to the forth frequency were included. Every graph is drawn for different FG indexes from pure metal to pure ceramic. These results have been calculated assuming that the temperature change is equal to zero, hub radius is zero, twist angle is 37 degrees and plate's dimension is  $\frac{a}{h} = 30$ . When the angular velocity increases, the amount of non-dimensional frequency increases for all of mode numbers. By increasing in amount of mode number, it is expected that frequency increases due to wavelength increase. This is shown in the Fig. 2 clearly. This increase is resulted from increasing the rotary inertia. Increase the frequency of pure ceramic plate is more

considerable than that for FGM or pure ceramic plates. The reason of this behavior is that, when the phase changes from metal to ceramic, the stiffness of the system increases. The increase in frequency is resulted from an increase in stiffness of the system.

Fig. 3 shows the effect of temperature change on non-dimensional frequency of functionally graded rotating plate in different angular velocities. Various mode numbers from fundamental frequency to the forth frequency were included. These results have been calculated with this assumption that the hub radius is equal to zero, plate dimension is  $\frac{a}{h} = 50$ , FG index is equal to 1 and twist angle is 37 degrees. Based on classical plate theory, increasing the value of  $\frac{a}{h}$  causes that the extracted results would be more realistic. The reason of this behavior is that, some effects have been neglected in the classical plate theory; for example, transverse deformations are more effective at smaller amounts of  $\frac{a}{h}$ . At the fundamental frequency, the behavior of plate vibration is different from other cases. This difference in results is due to special selected boundary conditions. Previous articles have shown that the response

Table 4 The effect of various aspect ratios, FG index and thermal change on non-dimensional fundamental and second frequency

Aspect ratio	FG index	Fundamental frequency				Second frequency			
		$\Delta T = 0$	$\Delta T = 15$	$\Delta T = 30$	$\Delta T = 45$	$\Delta T = 0$	$\Delta T = 15$	$\Delta T = 30$	$\Delta T = 45$
0.5	Pure ceramic	3.989	4.115	4.248	4.391	6.373	6.369	6.368	6.373
	FG, $n = 1$	3.173	3.298	3.435	3.585	4.969	4.975	4.987	5.006
	Pure metal	2.710	2.823	2.952	3.097	4.174	4.192	4.220	4.262
1	Pure ceramic	3.908	4.026	4.149	4.280	9.188	9.105	9.020	8.934
	FG, $n = 1$	3.096	3.212	3.337	3.473	6.740	6.659	6.576	6.489
	Pure metal	2.631	2.736	2.854	2.985	5.267	5.194	5.119	5.040
2	Pure ceramic	4.006	4.072	4.136	4.200	15.835	15.742	15.646	15.54
	FG, $n = 1$	3.180	3.225	3.279	3.341	11.408	11.310	11.210	11.10
	Pure metal	2.698	2.733	2.7778	2.821	8.668	8.577	8.482	8.378

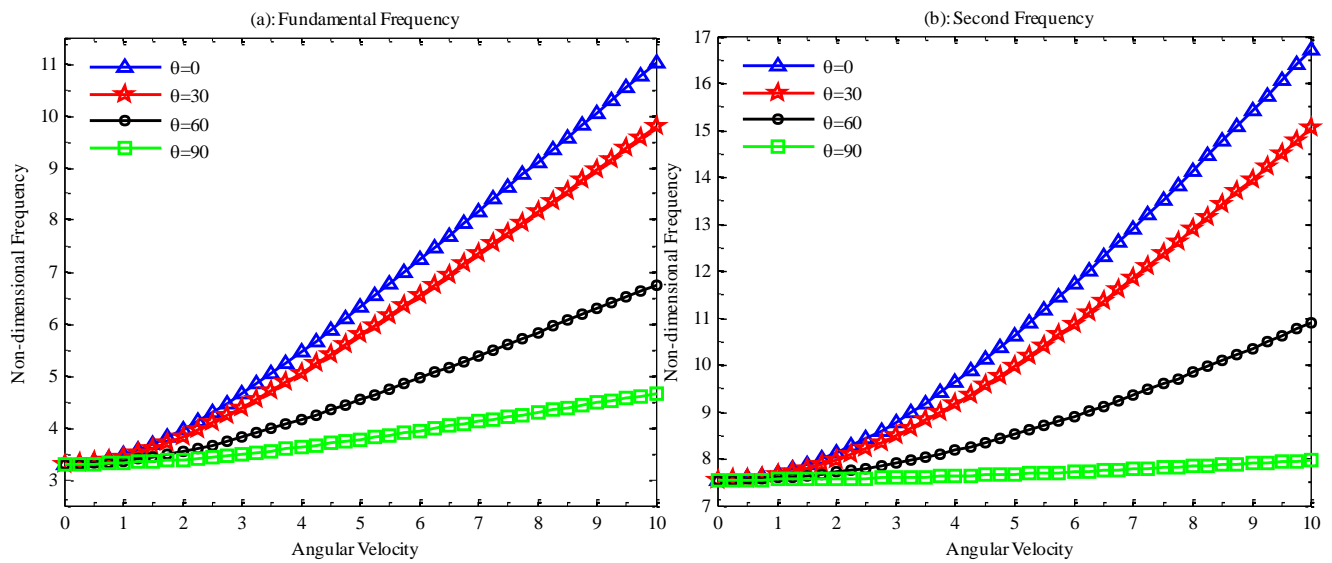


Fig. 4 The effect of various angular velocities on non-dimensional frequency in different twist angles

of fundamental frequency of a cantilever plate (i.e. with CFFF boundary conditions) for different parameters is different from other boundary conditions. Fundamental frequency with a cantilever boundary condition has a unique behavior, for example, it increases with increasing the rate of the cross-section (Huang and Li 2010) and increasing nonlocal parameters at the nonlocal theory (Aranda-Ruiz *et al.* 2012), or decreases with increasing the non-linear amplitude (Ghadiri and Shafiei 2015) and etc. These kinds of responses persuaded us to consider cantilever boundary condition in our investigation. In the case of fundamental frequency, it increases as the thermal change increases. But, other frequencies decrease as the thermal change increases. The non-dimensional frequency increases as the mode number increases from 2 to 4 and this predictable increase is resulted from the reduction in amplitude of transverse deformation of the plate in higher mode numbers.

Table 4 shows the effect of different aspect ratios in the first and the second mode numbers of non-dimensional frequency, different thermal changes and different FG indexes. In all cases of the fundamental frequency, when the

thermal change increases, the amount of frequency increases and in the second frequency, it decreases as the thermal change increases. And also, frequency increases as the aspect ratio increases. This table clearly shows that the frequency of pure ceramic plate is larger than frequency of FGM plate in all states. FG index increase causes stiffness of the system decreases, and it also causes the reduction in frequency. This behavior can be obtained in this table. Meanwhile in this table it has been shown performance difference between ceramic and metal at thermal environments.

The effects of various angular velocities on non-dimensional frequency at different twist angles are presented in Fig. 4. This figure clearly shows that non-dimensional frequency increases as the angular velocity increases. This increase is correct in both the fundamental frequency and the second frequency. Of course the second frequency in this case is always larger than the fundamental frequency, because the blade twist angle is related to its angular velocity. When the blade does not spin, blade angle of twist does not have any effect on frequency but when the angular velocity increases, change in angle of twist affects

the rotational inertia and finally the frequency changes. So that, when the angle of twist changes from zero to 90, due to reduction of inertia, the frequency decreases. The most important effect of angular velocity can be seen when the twist angle of the plate is equal to zero. The effect of angular velocity decreases as the hub radius of the plate increases. These results have been calculated with assumption that thermal change is 25 C and hub radius is equal to zero. Meantime usually changes in twist angle happens due to creating smooth air flow lines but this change leaves bad effects on vibration of system.

## 6. Conclusions

Vibration of a rotating FGM plate under thermal loading has been studied in this paper. The governing equation derived from Hamilton's principle and the generalized differential quadratic method is used to solve the extracted equation. A general review of the paper shows a lot of contents such as importance of angular velocity, thermal change, FG index, angular velocity, hub radius, mode number and aspect ratio. The frequency increases as the angular velocity increases. The fundamental frequency increases as the thermal change increases but in larger mode numbers, frequency decreases as the thermal change increases. The frequency increases as the aspect ratio increases and also, the frequency increases as the twist angle decreases. The frequency increases as the angular velocity increases. The non-dimensional frequency of pure ceramic plate is larger than other states; in addition, all of these results have been calculated for the cantilever boundary condition. This paper results can be helpful for designers who work in the field of rotating systems, especially turbine blade's designs.

## References

- Aranda-Ruiz, J., Loya, J. and Fernández-Sáez, J. (2012), "Bending vibrations of rotating nonuniform nanocantilevers using the Eringen nonlocal elasticity theory", *Compos. Struct.*, **94**(9), 2990-3001.
- Bernardo, G.M.S., Damásio, F.R., Silva, T.A.N. and Loja, M.A. R. (2016), "A study on the structural behaviour of FGM plates static and free vibrations analyses", *Compos. Struct.*, **136**, 124-138.
- Ghadiri, M. and Shafiei, N. (2015), "Nonlinear bending vibration of a rotating nanobeam based on nonlocal Eringen's theory using differential quadrature method", *Microsyst. Technol.*, 1-15.
- Hong, C.C. (2012), "Rapid heating induced vibration of magnetostrictive functionally graded material plates", *J. Vib. Acoust.*, **134**(2), 021019.
- Huang, Y. and Li, X.F. (2010), "A new approach for free vibration of axially functionally graded beams with non-uniform cross-section", *J. Sound Vib.*, **329**(11), 2291-2303.
- Huang, S.C. and Soedel, W. (1987), "Effects of coriolis acceleration on the free and forced in-plane vibrations of rotating rings on elastic foundation", *J. Sound Vib.*, **115**(2), 253-274.
- Ketabdari, M.J., Allahverdi, A., Boreyri, S. and Ardestani, M.F. (2016), "Free vibration analysis of homogeneous and FGM skew plates resting on variable Winkler-Pasternak elastic foundation", *Mech. Ind.*, **17**(1), 107.
- Lessia, A.W. (1969), *Vibration of plates*, NASA SP, p. 160.
- Li, L. and Zhang, D.G. (2016), "Free vibration analysis of rotating functionally graded rectangular plates", *Compos. Struct.*, **136**, 493-504.
- Malgaca, L., Al-Qahtani, H. and Sunar, M. (2015), "Vibration control of rotating blades using root-embedded piezoelectric materials", *Arab. J. Sci. Eng.*, **40**(5), 1487-1495.
- Park, J.S. and Kim, J.H. (2006), "Thermal postbuckling and vibration analyses of functionally graded plates", *J. Sound Vib.*, **289**(1), 77-93.
- Prakash, T., Singha, M.K. and Ganapathi, M. (2012), "A finite element study on the large amplitude flexural vibration characteristics of FGM plates under aerodynamic load", *Int. J. Non-Linear Mech.*, **47**(5), 439-447.
- Pandey, S. and Pradyumna, S. (2015), "Free vibration of functionally graded sandwich plates in thermal environment using a layerwise theory", *Eur. J. Mech.-A/Solids*, **51**, 55-66.
- Ramu, I. and Mohanty, S.C. (2015), "Free vibration and dynamic stability of functionally graded material plates on elastic foundation", *Defence Sci. J.*, **65**(3), 245-251.
- Shokrani, M.H., Karimi, M., Tehrani, M.S. and Mirdamadi, H.R. (2015), "Buckling analysis of double-orthotropic nanoplates embedded in elastic media based on non-local two-variable refined plate theory using the GDQ method", *J. Brazil. Soc. Mech. Sci. Eng.*, 1-18.
- Sofiyev, A.H. (2015), "On the vibration and stability of shear deformable FGM truncated conical shells subjected to an axial load", *Compos. Part B: Eng.*, **80**, 53-62.
- Sreenivasamurthy, S. and Ramamurti, V. (1981a), "A parametric study of vibration of rotating pre-twisted and tapered low aspect ratio cantilever plates", *J. Sound Vib.*, **76**(3), 311-328.
- Sreenivasamurthy, S. and Ramamurti, V. (1981b), "Coriolis effect on the vibration of flat rotating low aspect ratio cantilever plates", *J. Strain Anal. Eng. Des.*, **16**(2), 97-106.
- Subrahmanyam, K.B. and Kaza, K.R.V. (1986), "Vibration and buckling of rotating, pretwisted, preconcave beams including Coriolis effects", *J. Vib. Acoust. Stress Reliabil. Des.*, **108**(2), 140-149.
- Tornabene, F., Fantuzzi, N., Viola, E. and Reddy, J.N. (2014), "Winkler-Pasternak foundation effect on the static and dynamic analyses of laminated doubly-curved and degenerate shells and panels", *Compos. Part B: Eng.*, **57**, 269-296.
- Tornabene, F., Fantuzzi, N., Viola, E. and Batra, R.C. (2015a), "Stress and strain recovery for functionally graded free-form and doubly-curved sandwich shells using higher-order equivalent single layer theory", *Compos. Struct.*, **119**, 67-89.
- Tornabene, F., Fantuzzi, N., Ubertini, F. and Viola, E. (2015b), "Strong formulation finite element method based on differential quadrature: A survey", *Appl. Mech. Rev.*, **67**(2), 020801.
- Wang, J.S., Shaw, D. and Mahrenholtz, O. (1987), "Vibration of rotating rectangular plates", *J. Sound Vib.*, **112**(3), 455-468.
- Wang, Z., Zhao, M. and Yang, J. (2015a), "A piezoelectric gyroscope with self-equilibrated coriolis force based on overtone thickness-shear modes of a lithium niobate plate with an inversion layer", *Sensors J., IEEE*, **15**(3), 1794-1799.
- Wang, Y.T., Luan, P.G. and Zhang, S. (2015b), "Coriolis force induced topological order for classical mechanical vibrations", *New J. Phys.*, **17**(7), 073031.
- Yang, J. and Shen, H.S. (2002), "Vibration characteristics and transient response of shear-deformable functionally graded plates in thermal environments", *J. Sound Vib.*, **255**(3), 579-602.
- Yin, S., Yu, T. and Liu, P. (2013), "Free vibration analyses of FGM thin plates by isogeometric analysis based on classical plate theory and physical neutral surface", *Adv. Mech. Eng.*, **5**, 634584.
- Yoo, H.H. and Pierre, C. (2003), "Modal characteristic of a

rotating rectangular cantilever plate”, *J. Sound Vib.*, **259**(1), 81-96.

Young, T.H. and Liou, G.T. (1992), “Coriolis effect on the vibration of a cantilever plate with time-varying rotating speed”, *J. Vib. Acoust.*, **114**(2), 232-241.

CC